Measurement Science and Technology

PAPER

Bi-core optical fiber for sensing of temperature, strain and torsion

IOP Publishing Measurement Science and Technology

Meas. Sci. Technol. **30** (2019) 035104 (7pp) https://doi.org/10.1088/1361-6501/ab035b

Bi-core optical fiber for sensing of temperature, strain and torsion

A B Lobo Ribeiro[1], **S F O Silva**[2], **O Frazão**[2,3] **and J L Santos**[2,3]

[1] Faculty of Health Sciences, University Fernando Pessoa, Porto, Portugal
[2] Centre of Applied Optics, INESC-TEC, Porto, Portugal
[3] Faculty of Sciences, Department of Physics and Astronomy, University of Porto, Porto, Portugal

E-mail: alobo@ufp.edu.pt

Received 29 October 2018, revised 28 December 2018
Accepted for publication 30 January 2019
Published 15 February 2019

Abstract

Bi-core optical fiber structures are studied for applications in sensing. In this paper, an analysis is performed on the spectral characteristics of light propagating in these fibers with central launching core illumination from a standard single mode fiber. Reflective and transmissive configurations are addressed. The characteristics of a reflective bi-core fiber structure for measurement of strain, temperature and absolute value of torsion are investigated and highlights for further research are presented.

Keywords: fiber optic sensor, Bi-core optical fiber, temperature sensor, strain sensor, torsion sensor

(Some figures may appear in colour only in the online journal)

1. Introduction

Fiber optic sensing derived initially from the optical fiber communication endeavour but soon followed its own driving force triggered by the intrinsic favorable properties of these fibers. At a basic level, they result from the fact an optical field is involved with its unique characteristics of being simultaneously a communication channel and a sensing element. This feature means no dedicated telemetry and power channels are required, which leads to the practical feasibility of remote sensing and multi-point measurement supported by a single optical fiber [1].

It is historically accepted that the first research work involving optical fiber sensing was published in 1967 by Menadier *et al* [2], in a development where it studied the efficiency of the light coupling into a collector fiber after exiting an illumination fiber and reflection on a surface; such efficiency depends on the surface distance to the fiber tips, thus the configuration is indeed a displacement sensor, emphatically designated as 'Fotonic Sensor' by the team that performed the study. In subsequent years, progresses in this new scientific area were modest, a situation that changed in the second half of the 1970s. In 1974, Powel [3] described two different optical displacement sensors using only a pair of large-diameter fibers and a bundle of many small-diameter fibers. In 1976, Vali *et al* [4] presented a communication demonstrating that the sensitivity of an optical fiber ring interferometer can be considerably increased when the number of fiber loops is higher, illustrating the huge potential of fiber optic based interferometric sensing. In a famous development, Bucaro *et al* [5] in 1977 demonstrated, for the first time, the optical fiber hydrophone, supported by a Mach–Zehnder interferometric configuration with optical fiber arms. The following years framed the stabilization of the optical fiber sensing concept and an increasing number of novel and ingenious sensor structures and systems targeting a variety of measurands appeared in the literature, in a movement that extended vigorously up to the present complemented by multiple initiatives and enterprises aiming the economic valorisation of this technology.

Nowadays, fibers with special cross-section geometries are of great importance in optical fiber based R&D and applications. Indeed, since the first publication by Knight *et al* [6] in 1996 on photonic crystal fibers (PCF), the optical fiber community has been continuously engaged on the study of fiber structures with lattice of air holes running along its length; these structures show remarkable properties that support a large variety of novel optical fiber devices. The works published by Knight in *Nature* [7] and by Russell in *Science* [8] are important landmarks in this area that undertook in the last decade a huge development, boosted not only by the demands

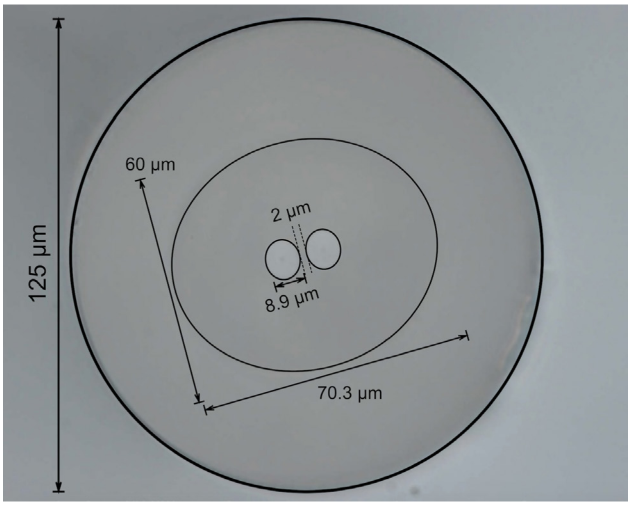

Figure 1. Photo of the cross-section of the bi-core fiber with physical dimensions superimposed ($w = 2$ µm, $2a = 8.9$ µm).

of optical fiber communication [9] but also in face of the large potential this technology has for sensing [10]. Surely, before the outcome of micro-structured optical fibers the conception of optical fiber sensing systems was constrained by a rather limited flexibility in optical fiber design and fabrication. Indeed, and in general, these systems had to be worked out around standard optical fibers with the consequent poor level of flexibility. Although, some exceptions existed as is the case of birefringent optical fibers that constituted the platform of many important sensing developments that have been reported along the years since the pioneer work of Eickhoff in 1981 [11]. However, probably the most notable example of structured optical fiber prior the photonic crystal fiber era is the bi-core fiber (also known as dual-core fiber or twin-core fiber). The concept was reported in by Meltz and Snitzer [12, 13]. In the 2nd International Conference on Optical Fiber Sensors, Berlin 1984, Noda *et al* [14] reported results on the application of bi-core fibers for twist angle measurement.

By the end of 80s, Peter Severin at the Philips Research Labs, Eindhoven, Netherlands, did a systematic study of these fibers emphasizing their potential for multi-purpose evanescent mode coupling based devices, in particular for sensing [15, 16]. Somehow surprisingly, during the 90s the consideration of these fibers for sensing was rather limited, eventually due to the focusing of the R&D community that operates in this field on fiber Bragg grating based sensor structures, a very hot topic by the time. The interests in bi-core fibers (more generally, in multi-core fibers) reappeared strongly in the last decade, but now in the context of microstructured optical fibers and few studies were reported on sensing configurations supported by classical bi-core fibers, certainly with some exceptions as is the case of the flow velocity sensor reported by Yuan *et al* [17] and refractive index sensor report by Guzmán-Sepulveda *et al* [18].

In this work, we recover the study of these fibers looking for their application as sensing structures. First, a simple model that provides insight on light propagation in bi-core fibers under central illumination is detailed, then the spectral characteristics of a fiber layout based on a length of bi-core

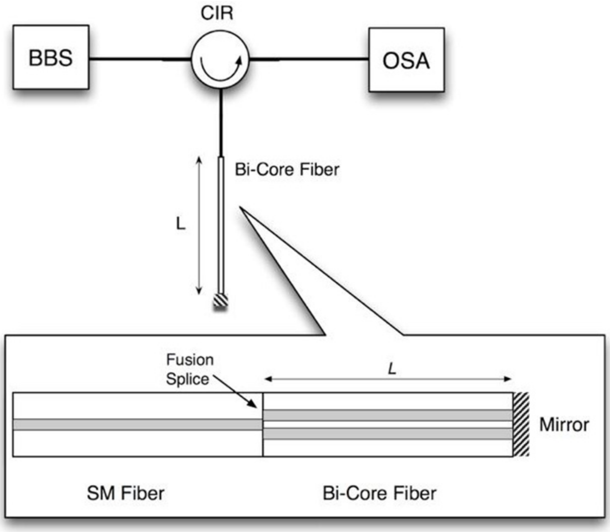

Figure 2. Schematic diagram of the sensing head in reflection. The legend: BBS: broadband source; OSA: optical spectrum analyzer; CIR: fiber optic circulator..

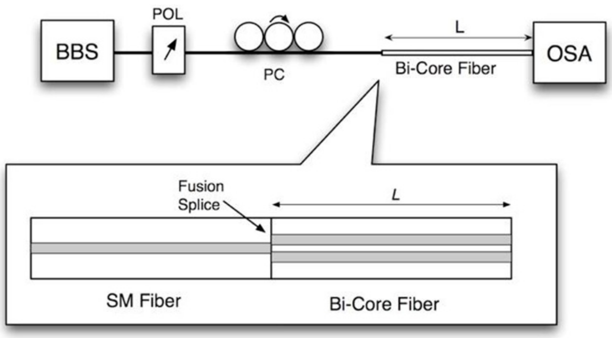

Figure 3. Schematic diagram of the sensing head in transmission. The legend: BBS: broadband source; OSA: optical spectrum analyzer; POL: in-fiber linear polarizer; PC: fiber coils polarization controller.

fiber with input and output leads in standard SMF fiber are experimentally investigated considering both transmission and reflective configurations, and in a third part, the properties of these structures for the measurement of mechanical strain, temperature and torsion are addressed.

2. Methods

2.1. Light excitation of bi-core fibers

In any electromagnetic wave guiding device, the electromagnetic waves are propagated in modes: these modes can exist depending on the boundary conditions and waveguide material properties, which modes are excited depend on the launching conditions, and upon propagation the mode spectrum may change so that the modes with lowest loss dominate. In general, the mode more confined to the center of the waveguide shows the lowest loss.

In bi-core fiber (BCF) sensing devices, two types of launching conditions are normally considered. Most studies [19, 20]

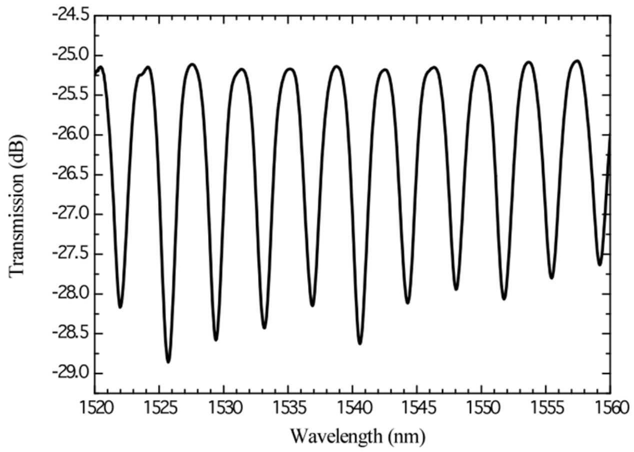

Figure 4. Spectral response of the BCF reflection configuration ($L = 540$ mm).

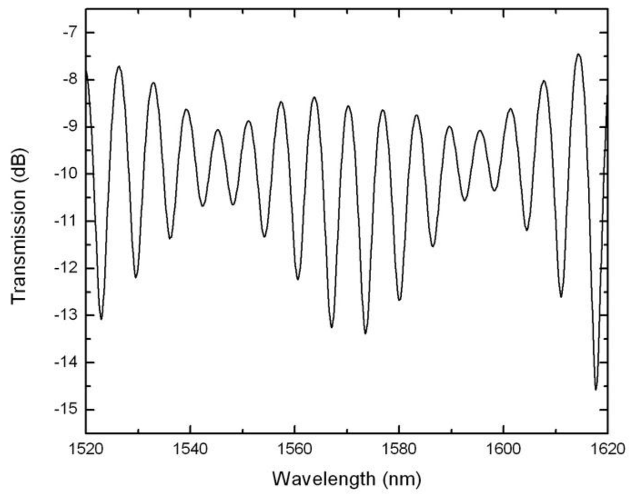

Figure 5. Spectral response of the BCF transmission configuration ($L = 450$ mm is reduced due to the cut-&-splice).

refer to launching light in one fiber core only and determining the effects of evanescence mode coupling over the space left between the two cores, generally a fraction of the fiber cores radius. The other possibility is central launching, the one that will be analyzed here. It is implemented by launching light into the two cores simultaneously from one connected single-mode fiber, thus covering the central space and two roughly half-moon sections of the fiber cores. For the present study, the two cores are assumed to be identical, circular, at equal distance from the axis and uniform over the length used. Surely, the manufacturing of a glass-preform from which a BCF is to be drawn is a highly delicate process and there is always a level at which the fiber is found imperfect and departures from the ideal situation are noticeable.

An approximation for the BCF consists in considering it as a step-index fiber propagating the two lowest order modes and with a super-core radius A, given by

$$A = 2a + w \tag{1}$$

where a is the radius of the cores and w the separation between them. The symmetric mode of the BCF is not a proper mode of the super-core, but it can be approximated to the LP_{01} mode

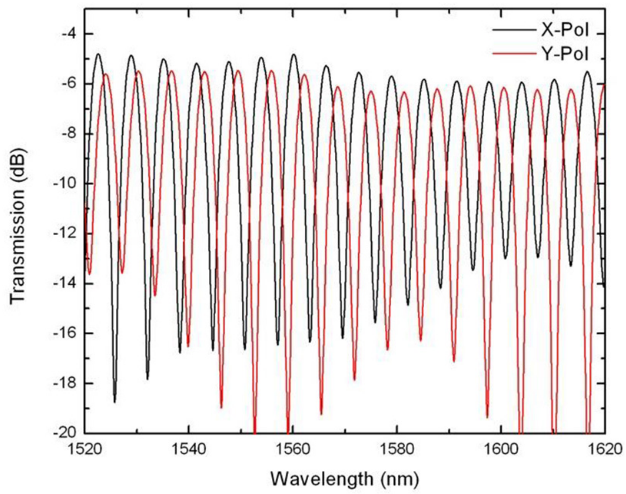

Figure 6. Spectrum of the light exiting the BCF operated in transmission for polarized light along the principal birefringent axis of the fiber.

of the super-core assuming it induced a field reduction in the region between the two cores (this approximation is very effective when the target is the mode propagation constant and not the mode field profile). On the other end, the asymmetric mode of the BCF is indistinguishable from the LP_{01} mode of the super-core.

The propagation constant, β, of the modes in a step-index fiber depends on the principal mode number, m, by

$$\beta \approx n_1 k_0 \left[1 - \Delta\left(\frac{m}{M}\right)^2\right] \tag{2}$$

where $k_0 = \frac{2\pi}{\lambda_0}$ is the wave number, being λ_0 the wavelength of the light in vacuum, $\Delta \equiv \frac{n_1 - n_2}{n_1}$ with n_1 and n_2 being the fiber core and cladding refractive indexes, respectively; $M = ak_0 n_1\sqrt{\Delta}$ is the maximum value of the principal mode number m [16], with a the radius of the core (in the present case, $a = A$). In equation (2), the principal mode number $m = 0$ is associated with the mode LP_{01} and $m = 1$ with the mode LP_{11}. Therefore,

$$\Delta\beta \equiv \beta_{LP_{01}} - \beta_{LP_{11}} \approx \frac{1}{A^2 k_0 n_1}. \tag{3}$$

The BCF used in this work was fabricated at the Philips Research Laboratories in Eindhoven, Netherlands, and has the profile and dimensions shown in figure 1.

From it comes $A = 10.9$ μm and substituting into (3) with $n_1 = 1.5$ results $\Delta\beta \approx 893\lambda_0$ mm^{-2}. Therefore, it can be written in a more practical form:

$$\Delta\beta \equiv \left(\frac{1}{2\pi A^2 n_1}\right)\lambda_0 + C = B\lambda_0 + C \tag{4}$$

and C is a constant that may be required in view of the approximations introduced. At the end of the BCF of length L the output light from the two modes will interfere constructively when

$$L\Delta\beta = 2\pi i; \quad \text{with } i = 0, \pm 1, \pm 2, \ldots. \tag{5}$$

From (4) the phase difference after a propagation length L is given by

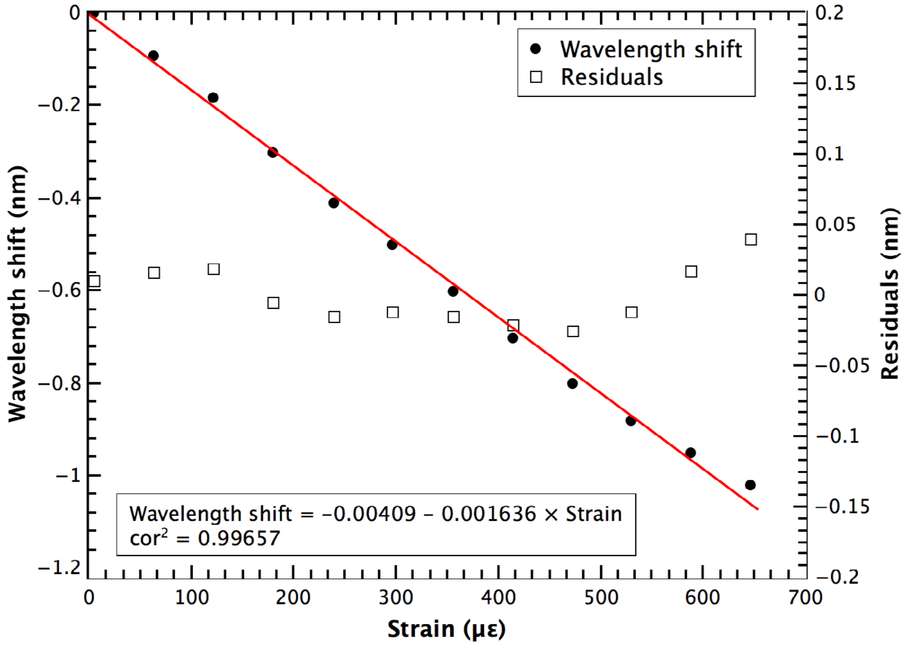

Figure 7. Sensor response under axial strain variation and the residual to the linear fit.

$$\Delta\phi = L\Delta\beta = BL\lambda_0 + CL. \tag{6}$$

The phase variation of $\Delta\phi$ with the wavelength is then

$$\delta(\Delta\phi) = BL\delta(\lambda_0). \tag{7}$$

Two successive peaks in the channeled spectrum means $\delta(\Delta\phi) = 2\pi$, associated with a wavelength periodicity, $\delta(\lambda_0)_{2\pi}$, given by

$$\delta(\lambda_0)_{2\pi} = \frac{2\pi}{BL} = \frac{4\pi^2 A^2 n_1}{L}. \tag{8}$$

2.2. Bi-core fiber sensor configurations

The spectral characteristics of light propagating in BCF with standard input/output fibers were experimentally studied considering the reflective and transmissive configurations.

2.2.1. Sensor configuration in reflection. The experimental setup for testing the central launching is shown in figure 2. An Er-doped fiber ASE broadband source (BBS) emitting depolarized light with central wavelength around 1550 nm and 100 mW average optical output power was used to illuminate the BCF through a 3-port fiber optic circulator. A fusion splice was done between a standard single-mode fiber (SMF) and the BCF that has a physical length (L) of ~540 mm. At this splice point, the optical power from the SMF is coupled equally into both cores of the BCF, propagates and couple between both cores over the length L, and are reflected back at the BCF end. This fiber end is silver mirror coated by chemical deposition process. The reflected optical power is partially coupled back into the core of the SMF at the same splice point and detected by the optical spectrum analyzer (OSA) via the 3-port fiber optic circulator (CIR). The length of the BCF (acting as sensor head) was fixed at both ends and kept straight between two precision rotation stages used to induce later on a controllable torsion about its longitudinal axis.

2.2.2. Sensor configuration in transmission. The layout for the transmissive configuration is shown in figure 3, which was also used to study polarization effects. Because the BCF geometry has two well-defined axes, the device must show dependence on the direction of polarization of the launched light. The plane of the axes of the two cores is associated with the horizontal (x) polarization, the direction perpendicular with the (y) polarization. The in-fiber linear polarizer (POL) and the fiber coil polarization controller (PC) permit to inject polarized light into the BCF with adjustable orientation. In this transmissive configuration, the BCF (acting as sensor head) had a physical length of ~450 mm (this reduced value, when compared with the reflective configuration, was due to cut-&-splice procedures necessary to change for transmissive configuration).

3. Results and discussion

3.1. Sensor configuration in reflection

Figure 4, shows the output-channeled spectra of the set-up configuration of figure 2 measured with the optical spectral analyzer (OSA). The wavelength separation between the maxima referred in equation (5) is $\delta(\lambda_0)_{2\pi} \approx 3.62$ nm (obtained from the measured spectral separation of ~29 nm between the eight peaks from the maxima 1528 nm to the one at 1557 nm). Using this value in equation (8) and considering the need the BCF

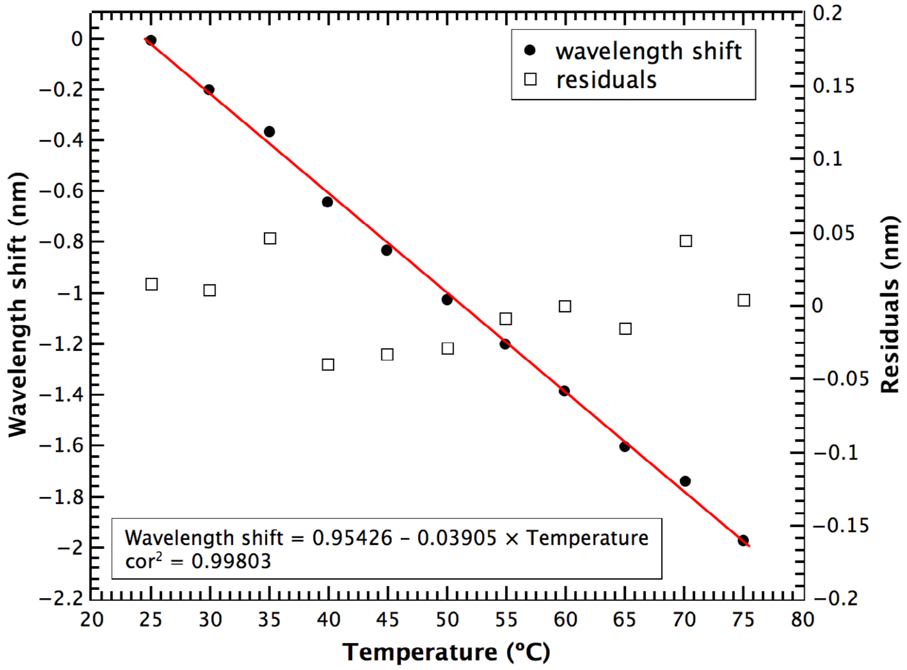

Figure 8. Sensor response under temperature variation and the residual to the linear fit.

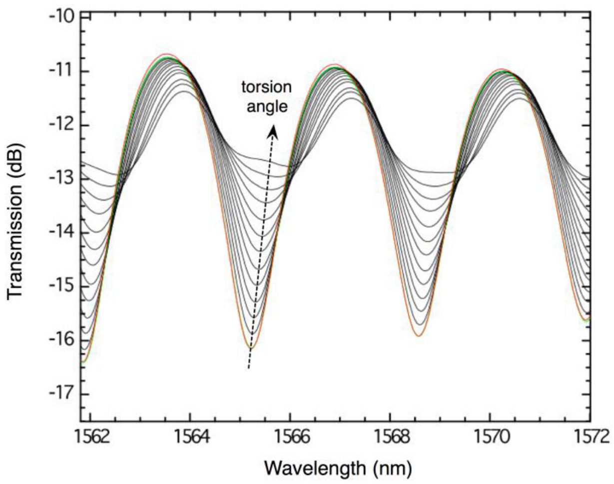

Figure 9. Sensor spectral response when torsion is applied (the dotted arrow shows the increase of torsion angle applied to the BCF).

length, $L = 540\,\text{mm}$, to be taken twice (because of the reflective configuration), it comes out a super-core radius value of $A \approx 8.1\ \mu\text{m}$. This value is smaller than the value $A \approx 10.9\ \mu\text{m}$ obtained from geometry shown in figure 1, but acceptable in view of the approximations introduced in the model discussed before.

3.2. Sensor configuration in transmission

The output-channeled spectrum from the transmissive configuration is shown in figure 5. Linear polarized light was launched in both fiber cores, but no particular effort was done to orientate the input light linear polarization with one of the birefringent axis. Consequently, it is expectable a substantial beating behavior, as indeed is observed.

To check the polarization properties of the BCF, arrangements were done in order to align the input linear polarization with each of the fiber birefringent axis. They relied on getting the two orthogonal polarizations at the input that resulted into minimum observable beating at the output channeled spectrum, also associated with the largest spectral difference between maximums of same order for the two polarizations.

Figure 6 shows the spectra obtained. The wavelength periods are $\delta(\lambda_0)_{2\pi|X} \approx 6.26\,\text{nm}$ and $\delta(\lambda_0)_{2\pi|Y} \approx 6.39\,\text{nm}$ for the x and y polarizations, respectively, indicating a birefringence for this fiber of $\approx 1.74 \times 10^{-5}$. Observation of the cross-section image of the fiber shown in figure 1 indicates this birefringence has geometric grounds not only because the BCF cross-section has two well-defined axes, but also in view of the elliptical shape of the cores with the minor axis fairly aligned with the line that connects the two cores.

3.3. Sensing effects

The dependence of the channeled spectrum shifts under the variation of strain, temperature and torsion was experimentally studied, looking for the application of this fiber structure as a sensing device. It is relevant to mention the sensing mechanism is the measurand induced shift of the phase difference between the light that propagates in the two fiber cores, therefore birefringence behavior, which introduces what can be mentioned as a second order effect, will not be considered under this study. The configuration with the BCF operating in reflection was selected (figure 2), with unpolarized light injected into the standard input fiber and $L = 540\,\text{mm}$. In the case of temperature measurements, the total length of the BCF was immersed on a water bath in order to have a better uniform distribution of temperature on the fiber. For the axial strain, both ends of the BCF were held on translation stages and displacement

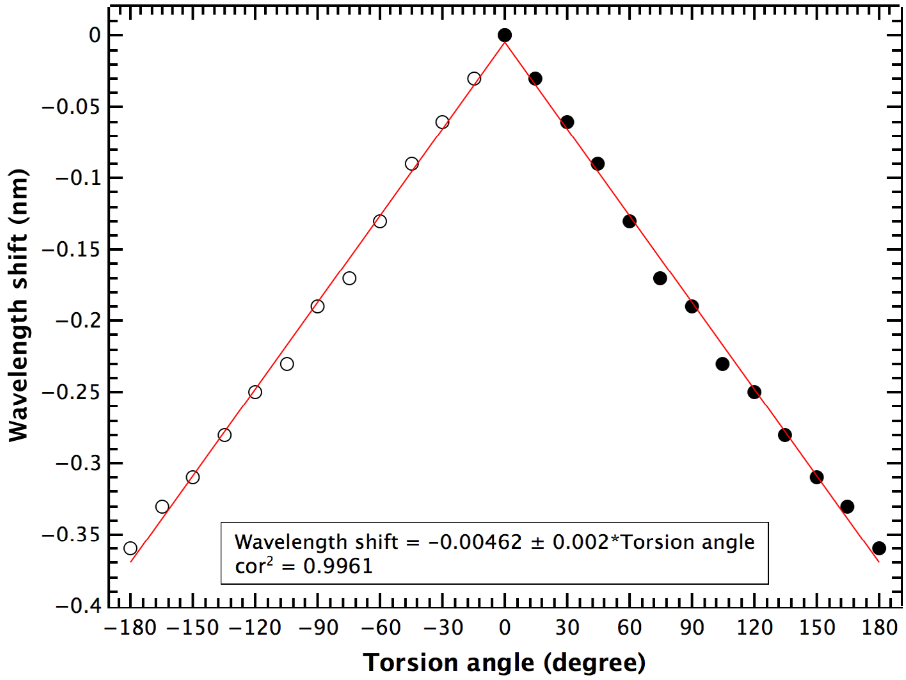

Figure 10. Sensor response when torsion is applied (the points between 0 and 180° are obtained from the graphs given in figure 9).

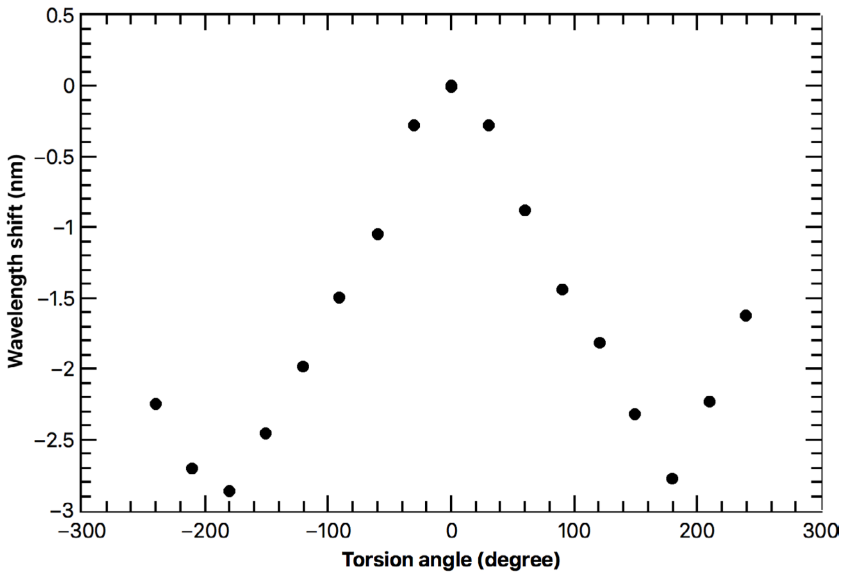

Figure 11. Sensor response when torsion is applied up to a torsion angle magnitude exceeding 180°.

was applied to one of them. The results obtained are shown in figures 7 and 8 for the cases of applied strain and temperature variations, respectively. Linear fitting dependences are observed with slopes (sensitivities) of $\frac{\Delta\lambda}{\Delta\epsilon} \approx -1.64\,\mathrm{pm}/\mu\varepsilon$ for strain and $\frac{\Delta\lambda}{\Delta T} \approx -39.1\,\mathrm{pm}/^{\circ}\mathrm{C}$ for temperature.

The effect of mechanical torsion on the fiber was also investigated. For that, a controllable torsion on the BCF was applied using two precision rotation stages. Figure 9 shows the evolution of the channeled spectrum in response to the torsion angle (anti-clockwise torsion). With increasing torsion angle the fringes are red-shifted and observed a decrease of the fringes visibility.

Choosing one the spectral dips on figure 9 (in this case ~1565 nm) and plotting the wavelength shift as function of the torsion angle, comes out the results given in figure 10, where now it is also shown the values obtained for clockwise torsion (0 to $+180°$). In both cases there is a red-shift of the spectrum, with a slope of approximately -2 pm/ldegreel, an expectable result by symmetry reasons.

For a larger range of torsion angles, figure 11 shows the results obtained, where in this case the length of BCF at the reflection setup configuration is ~990 mm. It is observed that with torsion angles larger than 180° the spectrum turns blue-shifted moving to recover the position without any torsion.

However, when the torsion angle increases, the interferometric visibility decreases (from a maximum value of ~52% to a minimum one of ~14%), while the peak optical power decreases by ~0.7 dB. Therefore, the torsion does not induce a substantial increase of the power loss in the BCF. These results indicate that it is feasible to measure torsion up to an amplitude of 180°, but without direct discrimination of clockwise and anti-clockwise torsion.

In all cases the measurand quantity information was obtained from the shift of the channeled spectrum obtained using an optical spectrum analyzer. This approach may not be adequate in several situations, either due to the cost of the equipment, limited reading resolution or bandwidth constraints. Therefore, it would be advantageous to consider a different interrogation approach and the white light technique combined with heterodyne demodulation [21] is a feasible alternative. In particular, it is well known for its characteristics of high sensitivity phase readout, which would translate, in the present case, into favorable sensitivities in the measurement of the targeted parameter.

It would be helpful to have available a model of the BCF sensing structure as a tool to estimate its performance when addressing the reading of a specific measurand, particularly the ones reported in this work and also curvature, as well as, to guide the optimization of the sensor. For that the approximated approach presented in section 2 is an insufficient basis and a more elaborated one is required. To our knowledge, that has not been done in the early days of this type of fiber applied for sensing, neither later after the outcome of photonic crystal fibers. Being true that nowadays the consideration of multicore fibers as sensor elements occurs most in the context of this new technology, in some circumstances keeps valuable the option associated with the utilization of standard bi-core fiers. Therefore, we consider worthwhile the development of such model, a subject of further research.

4. Conclusions

This work addressed the study of standard bi-core fibers in the perspective of sensing applications. The development of these special fibers in the context of the evolution of fiber optic technology was detailed, followed by a study performed on the spectral characteristics of light propagating in these fibers when illumination comes from a standard single mode fiber spliced centrally to the bi-core fiber. Reflective and transmissive configurations were considered and the characteristics of the former for measurement of strain, temperature and absolute value of torsion were studied.

Acknowledgments

The authors would like to express their gratitude and long term collaboration with Dr Peter J Séverin former senior research head officer at Philips Research Laboratories (Eindhoven, the Netherlands), and also, for providing us the bi-core optical fiber used in this work.

ORCID iDs

A B Lobo Ribeiro https://orcid.org/0000-0002-2988-1222

References

[1] Culshaw B 2004 Optical fiber sensor technologies: opportunities and—perhaps—pitfalls *J. Lightwave Technol.* **22** 39
[2] Menadier C, Kissinger C and Adkins H 1967 The fotonic sensor *Instrum. Control Syst.* **40** 114
[3] Powell J A 1974 Simple 2-fiber optical displacement sensor *Rev. Sci. Instrum.* **45** 302
[4] Vali V and Shorthill R W 1976 Fiber ring interferometer *Appl. Opt.* **15** 1099
[5] Bucaro J A, Carome E F and Layton M R 1977 Fiber ring interferometer optical fiber hydrophone *J. Acoust. Soc. Am.* **62** S72
[6] Knight J C, Birks T A, Russell P St J and Atkin D M 1996 All-silica single-mode optical fiber with photonic crystal cladding *Opt. Lett.* **21** 1547
[7] Knight J C 2003 Photonic crystal fibers *Nature* **424** 847
[8] Russell P St J 2003 Photonic crystal fibers *Science* **299** 358
[9] Cerqueira A 2010 Recent progress and novel applications of photonic crystal fibers *Rep. Prog. Phys.* **72** 024401
[10] Frazão O, Santos J L, Araújo F M and Ferreira L A 2008 Optical sensing with photonics crystal fibers *Laser Photonics Rev.* **2** 449
[11] Eickhoff W 1981 Temperature sensing by mode-mode interference in birefringent optical fibers *Opt. Lett.* **6** 204
[12] Meltz G and Snitzer E 1981 Fiber optic strain sensor *US Patent* No. 4295738(A)
[13] Meltz G, Dunphy J R, Morey W W and Snitzer E 1983 Cross-talk fiber-optic temperature sensor *Appl. Opt.* **22** 464
[14] Noda K, Taya H and Kimura T 1984 Twisting angle sensing using dual core fibers *Proc. 2nd Int. Conf. on Optical Fiber Sensors, OFS'84 (Berlin, Germany)*
[15] Severin P J and Bardoel W 1988 Evanescent-mode coupling in a bicore fibre: experiments and applications *Proc. SPIE* **949** 220
[16] Severin P J 1990 The bicore fibre, a multi-purpose evanescent mode coupling based device *Proc. SPIE* **1314** 348
[17] Yuan L, Yang J and Liu Z 2008 A compact fiber-optic flow velocity sensor based on a twin-core fiber Michelson interferometer *IEEE Sens. J.* **8** 1114
[18] Guzman-Sepulveda J R *et al* 2013 A highly sensitive fiber optic sensor based on two-core fiber for refractive index measurement *Sensors* **13** 14200
[19] Peng G D, Tjugiarto T and Chu P L 1994 Accurate elasto-optic probe method for measurement of coupling length in twin-core optical fiber *Appl. Opt.* **33** 1004
[20] Vallée R and Drolet D 1994 Practical coupling device based on a two-core optical fiber *Appl. Opt.* **33** 5602
[21] Caldas P *et al* 2009 Geometrical effects on the refractive index sensitivity of Mach–Zehnder fibre modal interferometers based on long-period gratings *Measur Sci. Technol.* **20** 075201